COLLEGE OF ENGINEERING

DEPARTMENT OF NUCLEAR ENGINEERING
LABORATORY FOR FLUID FLOW AND HEAT TRANSPORT PHENOMENA

Technical Report No. 18

CHOKED FLOW ANALOGY FOR VERY LOW QUALITY TWO-PHASE FLOWS

by:

Frederick G. Hammitt
M. John Robinson

Under contract with:

National Aeronautics and Space Administration
Grant No. NsG-39-60
Washington 25, D. C.

Office of Research Administration
Ann Arbor

March, 1966

ABSTRACT

Two theoretical models to predict axial pressure distribution, void fraction, and velocity in a cavitating venturi are applied. The theoretical predictions are compared with experimental data from cold water and mercury tests, and good agreement for the pressure profiles is found. The predicted void fractions are found to be too high, probably because the models assume zero slip or negative slip between the vapor and liquid phases.

The analogy between the cavitating venturi and other choked flow regimes is explored. One of the theoretical models used is based on the assumption that the cavitating venturi is essentially entirely analogous to a deLaval nozzle operating in a choked flow regime with a compressible gas.

The cavitating venturi is an example of an extremely low quality choked two-phase flow device. The present study is thus somewhat applicable to the study of liquid-cooled nuclear reactor pressure vessel or piping ruptures, which have received considerable attention in recent years. However, the qualities encountered in the present cavitation case are an order of magnitude lower than those usually considered for the reactor safety analyses, so that the present study is a limiting case for these.

ACKNOWLEDGMENTS

The authors would like to acknowledge the work of Dr. Willy Smith and Mr. Ian E. B. Lauchlan, former students at the University of Michigan, whose void fraction data was used for the comparisons with the theoretically derived numbers in this investigation, and Captain David M. Ericson Jr., USAF, doctoral candidate at the University of Michigan, whose experimental pressure profile data was used for this comparison with calculated pressure profile data.

TABLE OF CONTENTS

NOMENCLATURE

Symbol	Meaning
a,A	sonic velocity - area
B	ratio of vapor to liquid volume
f,F	fluid (subscript) - force
g_o,g	gravitational acceleration constant, g - vapor (subscript)
h	enthalpy
J	conversion constant - mechanical to heat energy units
k	thermal conductivity
L	liquid (subscript)
M,$\dot{m}$	Mach number, mass flow rate
P	pressure
R	universal gas constant
t,T	venturi throat (subscript) - total (subscript)
v	specific volume
V	velocity
x	quality
Γ	parameter defined eq. (3) of Appendix
ρ	density
z	axial distance from throat discharge in venturis

LIST OF TABLES

LIST OF FIGURES

I. INTRODUCTION

Very low quality two-phase "choked" flows are important today in many applications. That which has received the greatest attention in recent years is the postulated nuclear reactor accident wherein a rupture of a high-temperature high-pressure liquid-carrying pipe is assumed. Another reactor safety problem also involving somewhat similar flow considerations is the occurrence of a rapid fuel temperature transient in a liquid-cooled core. In this case the evaluation of the maximum velocity of transport of the liquid-vapor mixture from the region becomes important.

Other applications of such low quality choked flows which have been of importance for many years are cavitating flow regimes such as exist in pumps, valves, marine propellors, hydraulic turbines, venturis and orifices, etc. The present data and analyses are motivated by these latter applications and hence involve extremely low qualities as compared to the usual reactor problem, since they deal with fluids such as low temperature water with its very low vapor to liquid density ratio. However, the void fractions are of a magnitude similar to those considered for the reactor cases. Hence the present study examines in detail the extremely low quality end of the spectrum from the viewpoint

of the reactor safety problems, which is, nevertheless, the primary area of concern in the usual cavitation situation.

The earliest studies which, to our knowledge, have considered the analogy between low-quality two-phase flows and the conventional compressible choked flows deal with cavitation (1,2). In both cases cavitating venturis were considered, as in the present study. In the paper by Hunsaker (1) it is noted that the maximum pressure rise occurs at the visual downstream termination point of the cavitation cloud. The Randall (2) paper discusses the use of the choked flow feature of a cavitating venturi for flow-rate regulation and notes that the flow region downstream of the throat exit consists of a high speed jet surrounded by vapor, a fact also noted by Nowotny (3). However, none of these presents a quantitative analysis of the flow such as the analogy to the conventional choked flow situations presented here.

The existence of a close analogy between cavitating flow phenomena in centrifugal or axial pumps and compressible flow phenomena in similar compressors has been realized for some time, including the facts that the occurrence of cavitation in a pump inlet was somehow very similar to the occurrence of Mach 1 conditions in a compressor inlet, and that both resulted in a choked flow condition. More quantitative approaches have been made in recent papers on cavitating flow in centrifugal or axial flow pumps in order to explain some of the peculiarities in the effects of the cavitation on the pump performance (4,5).

A recent excellent quantitative study of the flow of low quality air-water mixtures through a converging-diverging nozzle, (i.e., a

"venturi" from the viewpoint of cavitating (flows), has been made by Muir and Eichhorn (6). This reports on the existence of a compression shock when the flow is underexpanded, but presents no analysis of this shock. A study of low-quality flow of water through a similar geometry is reported by Starkman, et al (7). In this particular case the minimum qualities considered are in the 1 to 2 percent range, which is considerably above the range considered in the present paper. The existence of compression shocks under suitable conditions is mentioned, but no quantitative data thereon is presented other than the observation that the condensation shock is much less abrupt than the conventional normal shock in a compressible gas flow. Finally, a very recent experimental and theoretical study of water-nitrogen mixtures at about 50 percent void fraction by Eddington (8) deals with shock phenomena in this type of mixture.

The above studies, which have only been selected as typical, since many more exist in the literature (see bibliography of reference 5, e.g.), are motivated by conventional flow applications rather than nuclear reactor safety problems. However, various studies motivated by reactor safety also exist in the literature. Studies by Levy (9), Moody (10), and Min, Fauske, and Petrick (11) are typical. Generally these deal with simple converging (rather than converging-diverging) passages, since a converging opening better models a possible rupture of a pipe or pressure vessel. Hence they consider the choked flow analogy in the throat of the converging section, but do not concern themselves with shock waves which are only involved in the diverging

("supersonic") portion. Generally the qualities considered are greatly in excess of those of the present paper.

In addition to all the above, there has also been some recent interest (12) in the quite analogous situation of high-quality choked flows such as are encountered with saturated vapor expanded through a nozzle. In this case it has long been known that condensation shocks sometimes occur after the flow has attained a non-equilibrium sub-cooled condition due to the rapidity of the expansion. This type of flow situation is primarily applicable to turbines operating with saturated or wet steam inlet conditions.

II. BACKGROUND FOR PRESENT STUDY

Considerable experimental data has been gathered in the authors' laboratory on cavitating flow regimes in venturis both with water and mercury as test fluid. This data includes measurements of axial pressure profiles, velocity profiles using a micro-pitot tube, and void fraction distribution by gamma-ray densitometer, as well as high speed motion picture studies of the flow. A portion of the data relating to the void fraction and pitot tube measurements already appears in the open literature (13,14), while additional void fraction (15) and pressure profile data (16) has not yet been published. A full description of the closed loop venturi tunnel facilities both for water and mercury has already been given (17). However, the basic flow path design of the venturis used is shown for convenience in Fig. 1. A 1/2" diameter cylindrical throat of 2.35" length is located between nozzle and diffuser sections, each with 6° included angle for the portion adjacent to the throat. The diffuser continues at this cone angle out to almost the full pipe diameter.

With a wealth of experimental data in hand for this cavitating flow geometry it is desirable to develop an analytical model capable of predicting a priori the pressure profiles, velocities, temperatures, and void fractions which would be encountered once the required independent

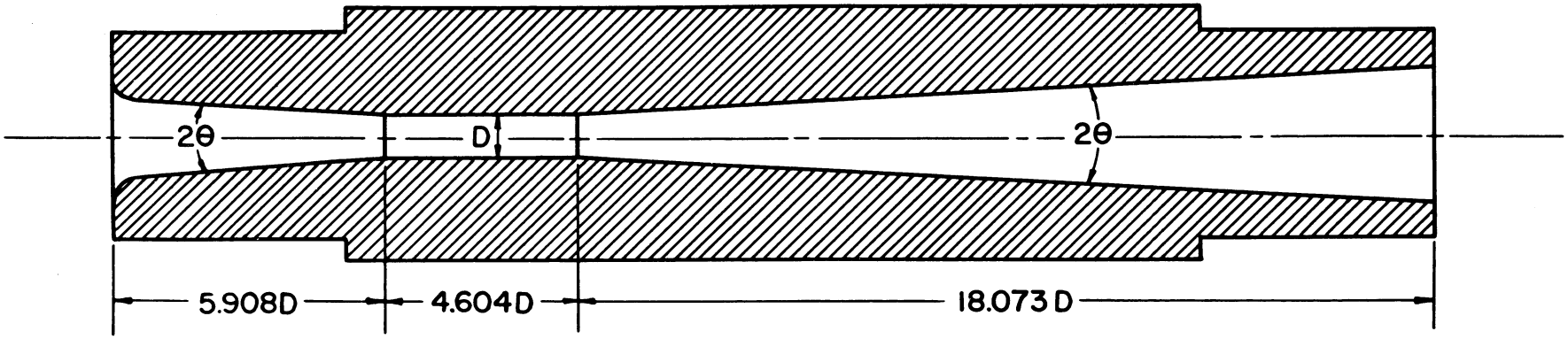

$$2\theta = \frac{5^\circ 54'}{6^\circ 04'}$$

1849

Fig. 1.--Basic venturi flow path dimensions.

variables had been set. While such a model applies primarily to the cavitating venturi case, it also has some application to other cavitating flows such as are encountered in turbomachinery, etc., and also to reactor safety problems, even though these may normally involve somewhat higher qualities than those considered for the present case (maximum of about 10^{-3}).

As already mentioned, earlier investigators (2,3) have noted that a cavitating venturi flow can often be considered approximately as a high speed central jet issuing from the throat and with a diameter and velocity approximately equal to those at the throat. Our own investigations with a pitot tube in water (18), by visual observation in mercury where the gap between the transparent wall and the central mercury column could easily be seen (13), and by gamma-ray densitometer void fraction measurement in mercury (13,14), tended to confirm the suitability of this model. However, later void fraction measurements in water (15), disagreed in showing a predominance of void fraction near the axis. The reason for the disagreement between the pitot tube and gamma-ray densitometer data in water is not known. However, the average void fractions presented as a function of axial position in Figs. 8 and 9 are taken from the gamma-ray densitometer data.

Two possible theoretical models for the flow were investigated. Neither matches the observations on the flow regime completely, but hopefully should give results of reasonable engineering accuracy.

i) Homogeneous flow model wherein it is assumed that the vapor is dispersed uniformly throughout the fluid for all planes normal to the

axis, that the two phases always have the same velocity, and that thermal equilibrium exists. The flow is assumed adiabatic everywhere, and isentropic except for the condensation shock wave which is assumed to exist at the termination of the cavitating region. The quality downstream of the shock is assumed to be zero. Conservation of momentum mass, and energy are satisfied for all cross-sections.

ii) Assuming the central jet model with diameter and velocity equal to those at the throat, it is assumed that the cavitation termination region is analogous to a hydraulic jump. The region around the central jet is assumed filled with stagnant vapor at a pressure equal to the saturation pressure existing at the throat discharge. While the "height" of the jump is terminated by the sidewalls of the venturi at their location, the pressure at the wall is assumed equal to that at the appropriate submergence if an actual hydraulic jump existed (see sketch of Fig. 2). In this model as applied to the conical venturi diffuser, gravity is neglected so that the wall pressure at the jump is assumed to apply over the entire cross-section. As in the conventional hydraulic jump analysis, momentum and mass are considered to be conserved across the jump. After the jump the liquid fills the entire cross-section, so that the quality here is zero as in the previous model. Note that the void fraction upstream of the jump is simply the ratio of area around the jet to total area for any cross-section.

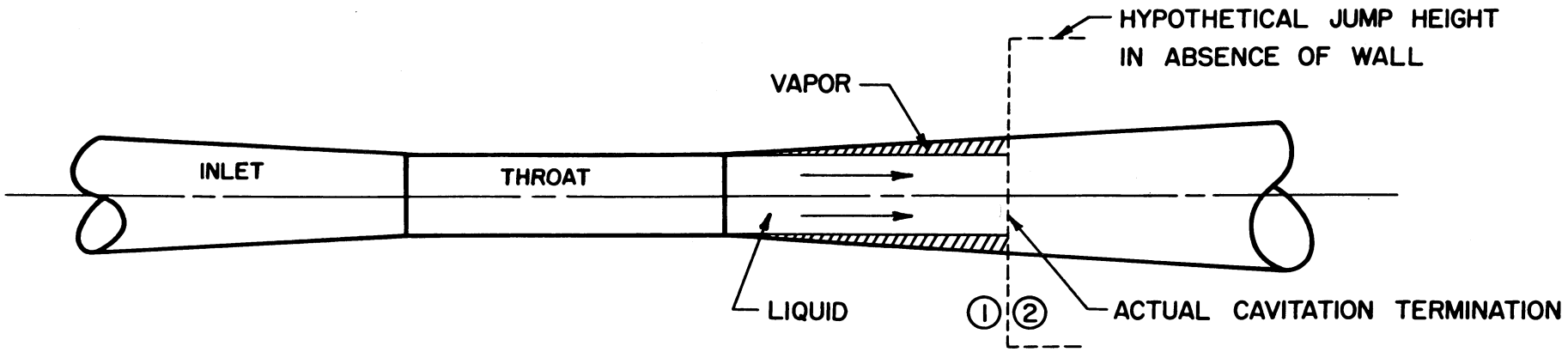

1858

Fig. 2.--Sketch of cavitating venturi hydraulic jump flow analogy.

III. CALCULATING PROCEDURES

The calculating procedures followed for the two models are summarized below:

A. Homogeneous Flow Model

1. Throat Discharge to Cavitation Termination Point

From the throat discharge to the cavitation termination point the flow is assumed to be isentropic-adiabatic. The throat velocity and water temperature at the throat can be considered independent variables, and hence known for a given case. Assuming that the flow is analogous to a compressible gas choked flow in a deLaval nozzle, Mach 1 must exist at the throat discharge where it is assumed that the cavitation will begin. Here, in a real case, the minimum pressure would be expected to exist for a cylindrical throat due to the effects of friction. In the present ideal flow analysis of course the pressure would remain constant along the throat. As shown in Fig. 3, sonic velocities in low quality water-steam mixtures can be extremely low (see Appendix for appropriate relations), and hence of the order of reasonable throat velocities for cavitating venturis, for void fractions in excess of 10^{-3}. Then, as shown in Fig. 4, the quality is of the order of 10^{-6} to 10^{-8}, and its net effect upon the thermodynamic mixture properties except for sonic

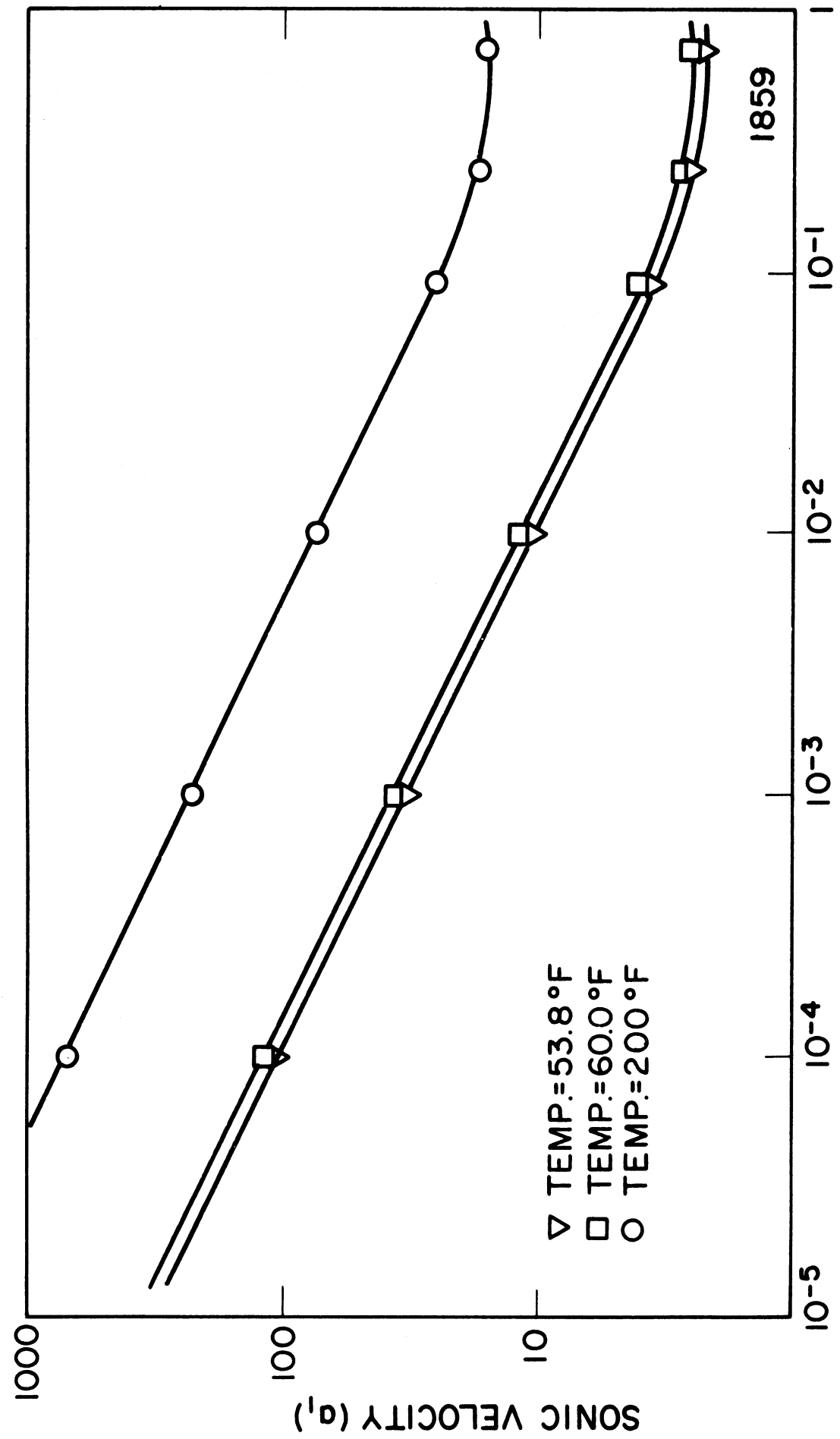

Fig. 3.--Calculated sonic velocity versus void fraction for homogenous mixtures.

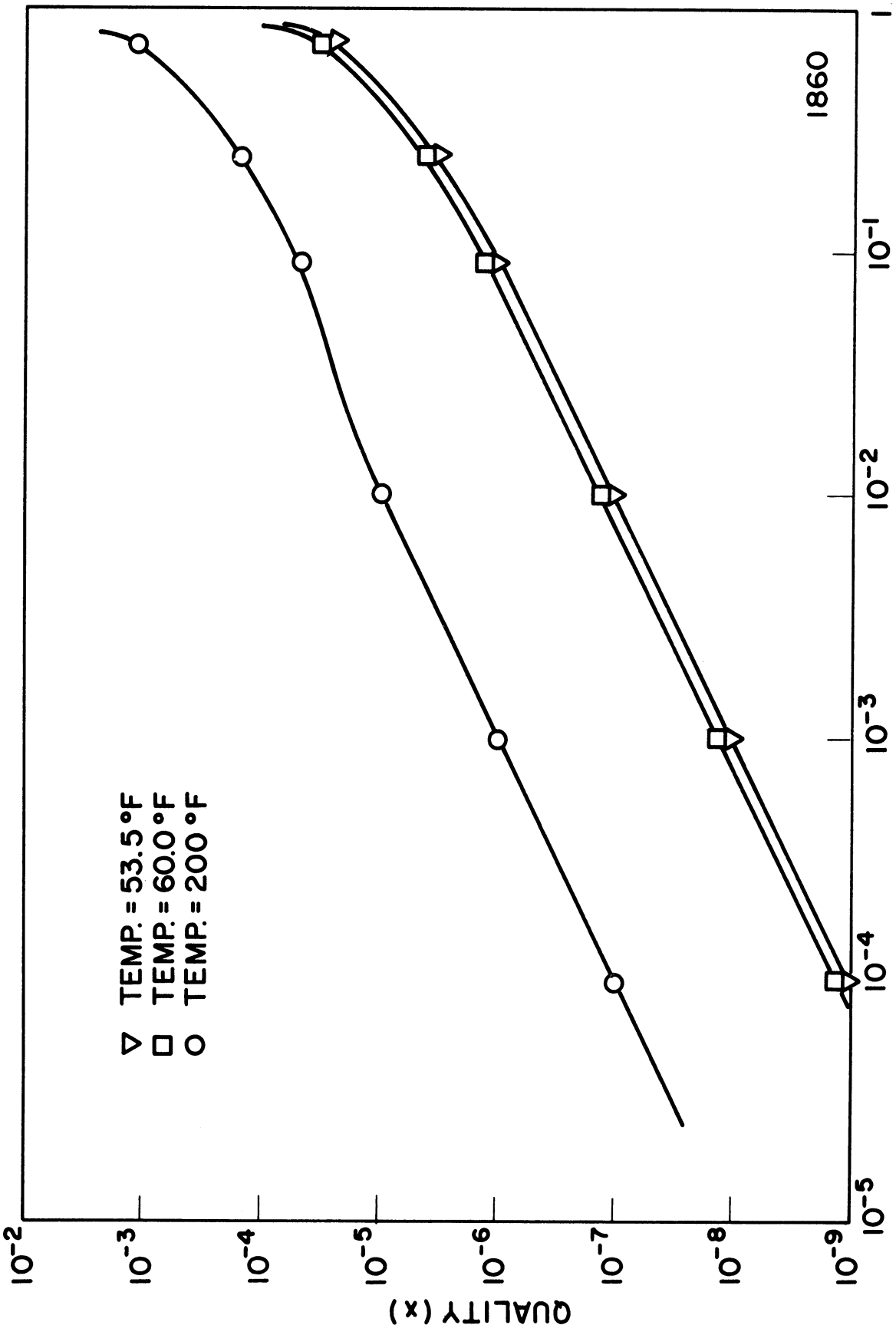

Fig. 4.--Calculated quality versus void fraction.

velocity is negligible. Hence the flow issuing from the throat can be considered pure liquid.

The computation of conditions for any point downstream of the throat discharge and within the cavitation region is entirely similar to that normally employed for the computation of conditions in a nozzle handling wet steam. Conventional steam tables (19) can be employed. The assumed process an a T-S diagram is sketched in Fig. 5, the region between t (throat discharge), and 1 (a point immediately upstream of the shock but in the cavitating region), being the portion under present discussion.

Using the steam tables (19), it is necessary to find by trial and error the temperature at point 1 such that the flow will remain isentropic, and the conditions of energy and mass conservation will be maintained (see Appendix for appropriate relations). For the cold water example computed (throat velocity of 64.6 ft./sec.), the temperature drop to the point of cavitation termination is only a very small fraction of a degree. This is typical of the cavitation case. Even so, this temperature decrease must be considered since the specific volume and entropy of the vapor are extremely sensitive to temperature in this region. Also, the velocity of the mixture is quite constant from the throat discharge to the cavitation termination point, with the void fraction increasing appropriately to counter the increase in cross-sectional area of the diffuser. The theoretical model for homogenized flow is thus consistent with the hypothesized central jet flow regime in that both predict relatively constant velocity through the cavitation region.

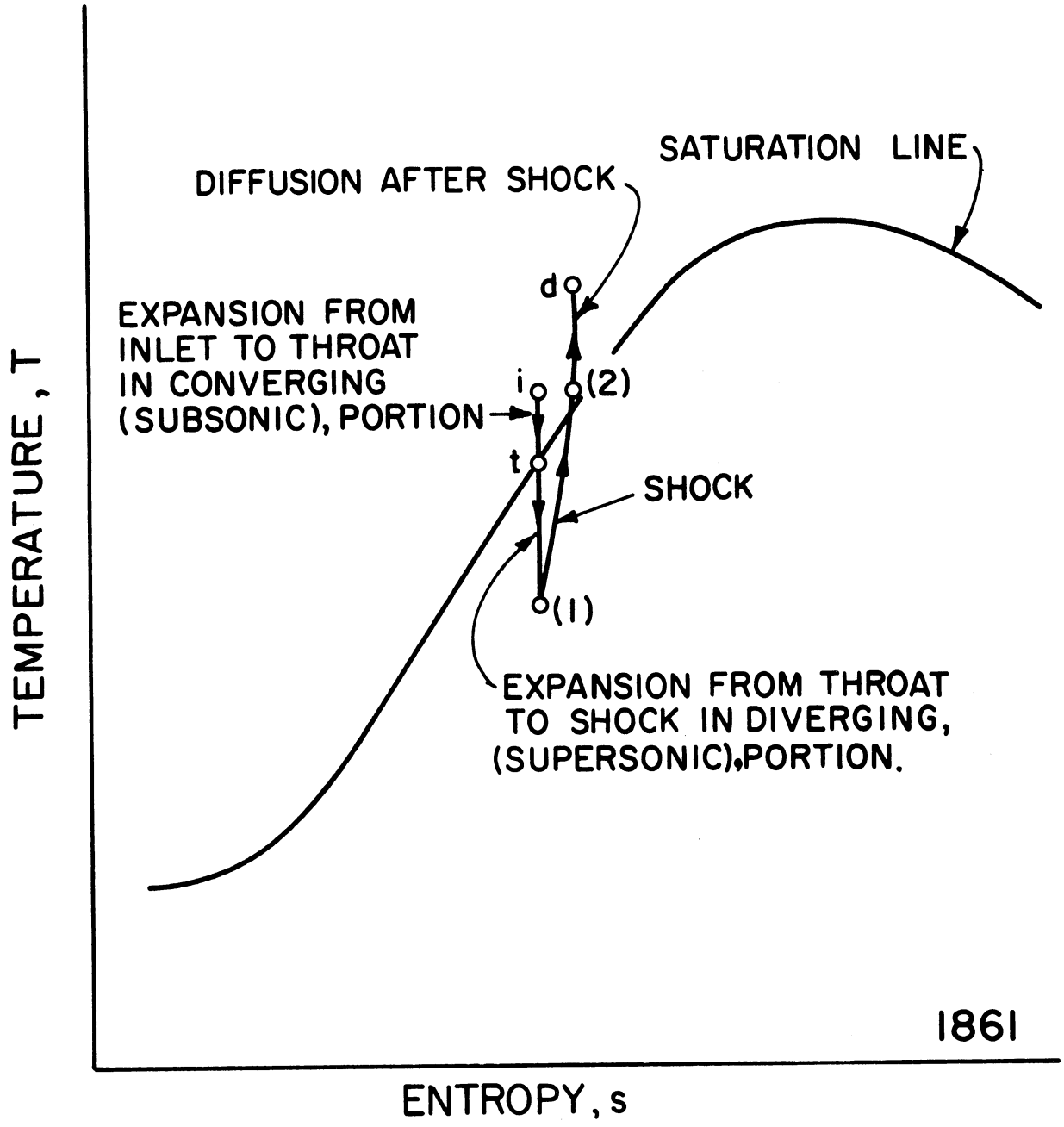

Fig. 5.--T-S diagram of the cavitating venturi process.

2. Cavitation Termination Region (Shock Wave)

The conditions immediately upstream of the postulated shock wave are as given from the calculation previously discussed. If the velocity of sound is computed for the mixture at this point, it is found that the flow is highly supersonic as would be expected from the analogy with compressible gas flow. It is required that immediately after the shock, which is assumed to require zero axial extent, all the vapor has condensed (Fig. 5), so that the quality and void fraction are zero. Thus it is clear that after the shock the flow is highly subsonic since the velocity of sound in a liquid is typically of the order of 10^3 to 10^4 feet per second.

After the shock the fluid may have a pressure in excess of vapor pressure for the new temperature, which is presumably slightly above the temperature upstream of the shock by virtue of the latent heat released by the condensing vapor. In fact it is clear that the enthalpy after the shock must be greater than that at throat discharge, since the kinetic head has decreased. In general, then, the temperature must also be higher since, while there was a slight quality at throat discharge, the fluid is assumed vapor free after the shock.

The calcuation of conditions after the shock from the upstream conditions requires an application of conservation of momentum and mass. The only quantity of interest to be found from conservation of energy is the temperature after the shock. However, sample calculations show that this quantity does not change appreciably over the shock. The conservation of mass and momentum equations can easily be arranged to the form

of eq. (6) and (7) in Appendix B, with the assumption that $x \ll 1$. Hence the validity of the theoretical results is limited to $x < 0.01$. Using these equations it is possible to make the calculation. However, in order to explore the analogy with compressible gas flow it was desired to express the relations in terms of Mach number. This can be accomplished as shown in Appendix A following to some extent the procedure of Jakobsen (4). The operative equations are now eq. (12), (13), and (14), and from these the conditions after the shock can be computed.

3. Cavitation Termination to Venturi Discharge

Since the flow in this region is vapor free, the computation is entirely straightforward and assumes frictionless flow. In terms of the T-S diagram (Fig. 5), this portion is an isentropic compression from 2 to d, where the liquid is subcooled.

B. Hydraulic Jump Model

1. Throat Discharge to Cavitation Termination

In this region a central liquid jet (zero quality) is assumed surrounded by stagnant vapor at the vapor pressure corresponding to throat discharge temperature. Temperature is assumed constant throughout. Since the jet diameter is assumed equal to the throat diameter, the jet velocity remains equal to the throat velocity. For this model the void fraction at any axial position within the cavitation region is simply the ratio of the cross-sectional area around the jet to the total cross-sectional area. This is also approximately true for the shock wave model since, at least for the examples computed, the velocity upstream of the shock is about equal to the throat velocity.

2. Cavitation Termination Region (Hydraulic Jump)

Conservation of mass and momentum is applied across the cavitation termination region as in the conventional hydraulic jump analysis (20) except that the pressure is assumed uniform across a plane normal to axis immediately upstream of the jump, i.e., gravity is neglected. The jump, as the shock wave, is assumed to require zero axial extent. The analogy to a hydraulic jump stems from consideration of a two-dimensional case wherein the venturi wall would be fictitiously removed, and the liquid allowed to assume the height downstream of the jump which it would attain if the flow were horizontal, and under the influence of gravity (Fig. 2).

The applicable equations are shown in Appendix C, the operative equations now being eq. (15) and (17). It is noted that the momentum equation, (16), is identical to the comparable momentum equation from the shock wave analysis, (7). Thus the models will give similar results if V_1 is the same in the two cases. In the cases for water flow which have been investigated, this is essentially true, even for the 200°F water (Table I and Figs. 6 and 7). Since the pressure rise predictions from the two models are almost identical for the cases examined, only one theoretical curve is shown in Figs. 8 and 9, where the experimental results and theory are compared. This equality of results between the models is also the case for void fraction, so that again only one theoretical curve is shown.

TABLE 1

CALCULATED PARAMETERS FROM SHOCK WAVE AND HYDRAULIC JUMP MODELS

Temperature	A_t/A_2	Void Fraction	x Quality	M_1/M_2	a_1 sonic vel.	$\frac{P_2-P_v}{V_f^2/2g_o}$ Shock Wave	$\frac{P_2-P_v}{V_f^2/2g_o}$ Hyd.Jump
53.5°F	0.292	0.708	2.58×10^{-5}	7.30×10^{3}	2.30	0.415	0.413
	0.754[a]	0.246	0.344×10^{-5}	2.57×10^{3}	2.43	0.373	0.371
	0.9091	0.0909	1.603×10^{-6}	1.48×10^{3}	3.64	0.171	0.1473
	0.9901	0.0099	1.000×10^{-7}	4.68×10^{2}	1.058×10^{1}	0.0198	0.0196
	0.9990	1.000×10^{-3}	1.000×10^{-8}	1.48×10^{2}	3.30×10^{1}	0.0	0.0020
	0.9999	1.000×10^{-4}	1.000×10^{-9}	4.68×10^{1}	1.048×10^{2}	0.0	0.0002
	--	0.0	0.0	1.00	4.895×10^{3}	0.0	0.0
	--	1.0	--	--	1.347×10^{3}	--	--
60.0°F	0.292	0.708	3.23×10^{-5}	6.50×10^{3}	2.60	0.409	0.413
	0.754[a]	0.246	0.43×10^{-5}	2.38×10^{3}	2.75	0.366	0.371
	0.9091	0.0909	1.33×10^{-6}	1.32×10^{3}	4.12	0.171	0.1473
	0.9901	0.0099	1.00×10^{-7}	4.18×10^{2}	1.20×10^{1}	0.0198	0.0196
	0.9990	1.0×10^{-3}	1.00×10^{-8}	1.32×10^{2}	3.74×10^{1}	0.0	0.0020
	0.9999	1.0×10^{-4}	1.00×10^{-9}	4.18×10^{1}	1.20×10^{2}	0.0	0.0002
	--	0.0	0.0	1.00	4.935×10^{3}	0.0	0.0
	--	1.0	--	--	1.355×10^{3}	--	--
200.0°F	0.292	0.708	1.198×10^{-3}	1.020×10^{3}	1.630×10^{1}	0.410	0.413
	0.754[a]	0.246	1.598×10^{-4}	3.74×10^{2}	1.722×10^{1}	0.365	0.371
	0.9091	0.0909	0.495×10^{-4}	2.08×10^{2}	2.538×10^{1}	0.161	0.1473
	0.9901	0.0099	1.0×10^{-5}	6.57×10^{1}	7.56×10^{1}	0.0197	0.0196
	0.9990	1.0×10^{-3}	1.0×10^{-6}	2.08×10^{1}	2.34×10^{2}	0.0	0.0020
	0.9999	1.0×10^{-4}	1.0×10^{-7}	6.57	7.42×10^{2}	0.0	0.0002
	--	0.0	0.0	1.00	4.872×10^{3}	0.0	0.0
	--	1.0	--	--	1.527×10^{3}	--	--

[a]This condition is for standard cavitation.

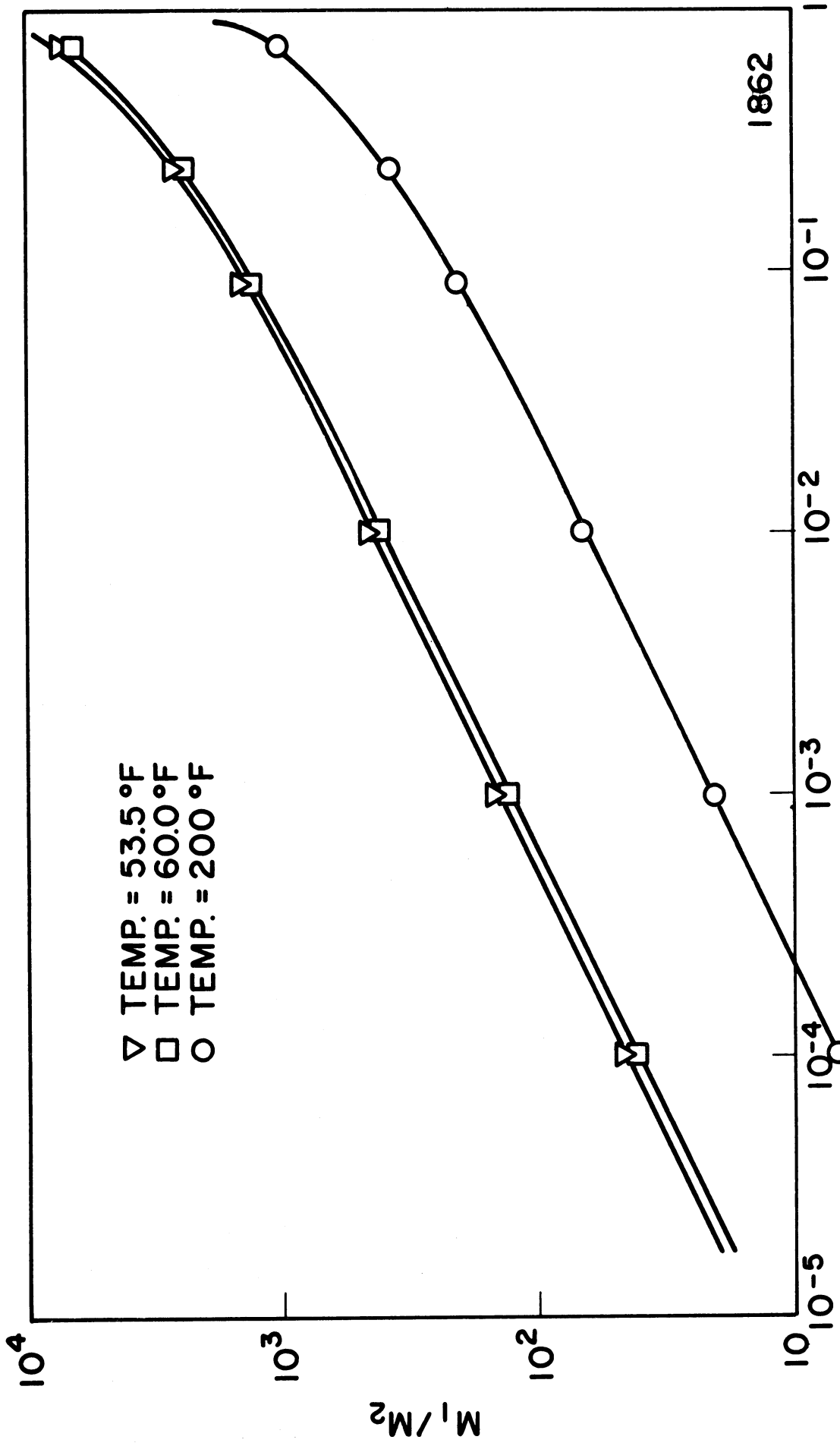

Fig. 6.--Mach number ratio for both models versus void fraction for both shock wave and hydraulic jump models.

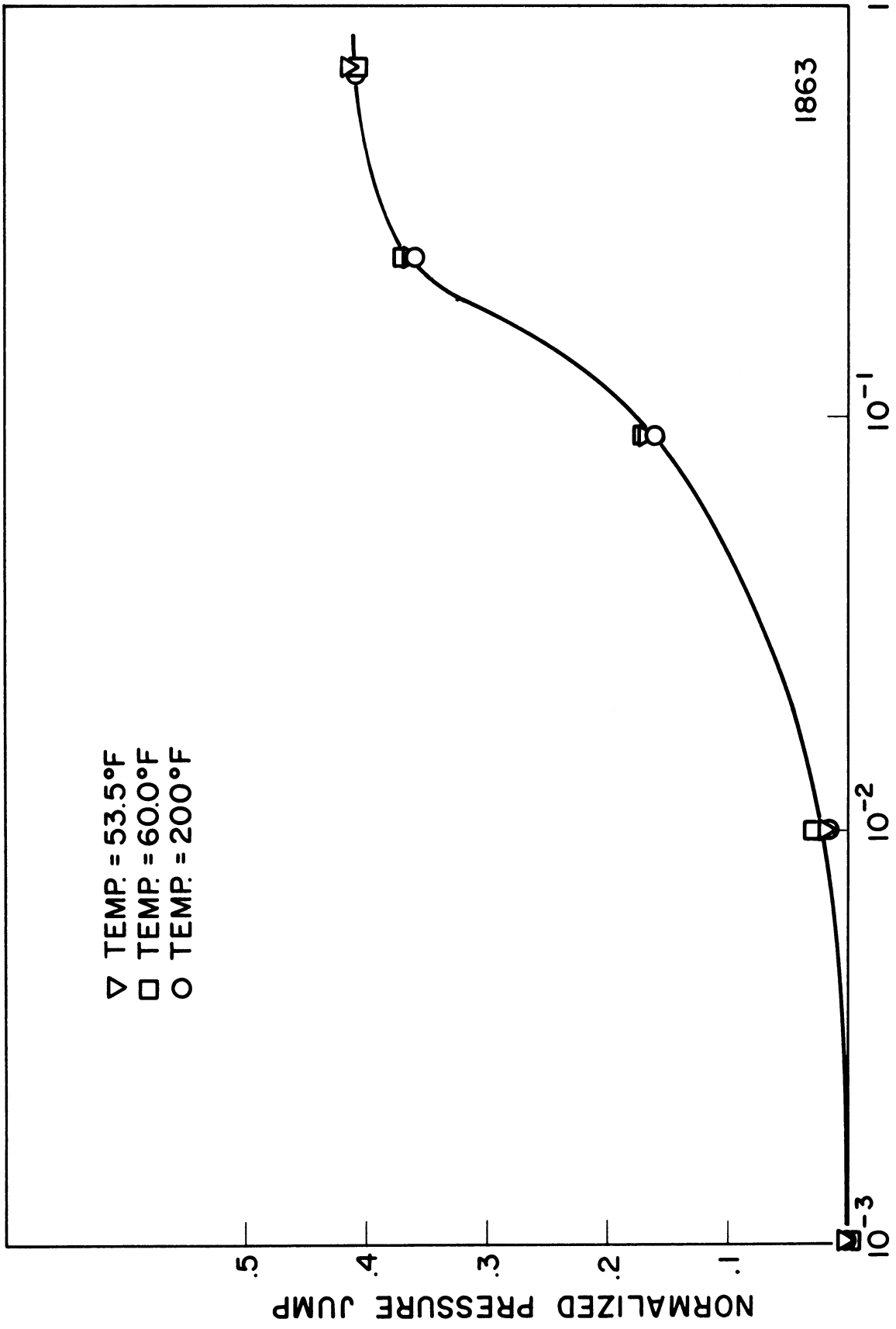

Fig. 7.--Calculated pressure jump versus void fraction for shock wave model.

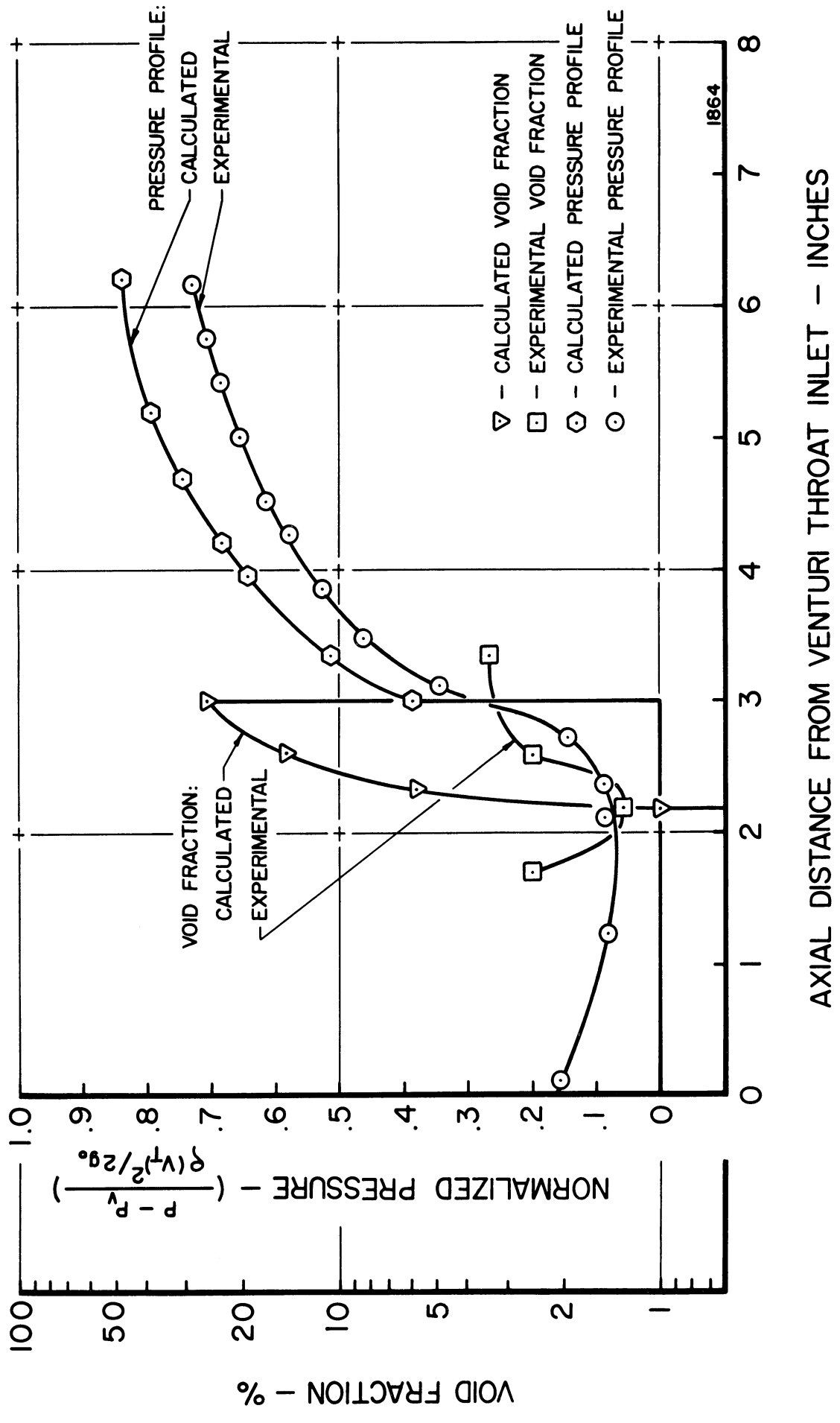

Fig. 8.--Normalized pressure and void fraction versus axial position for water, experimental versus calculated comparison for standard cavitation.

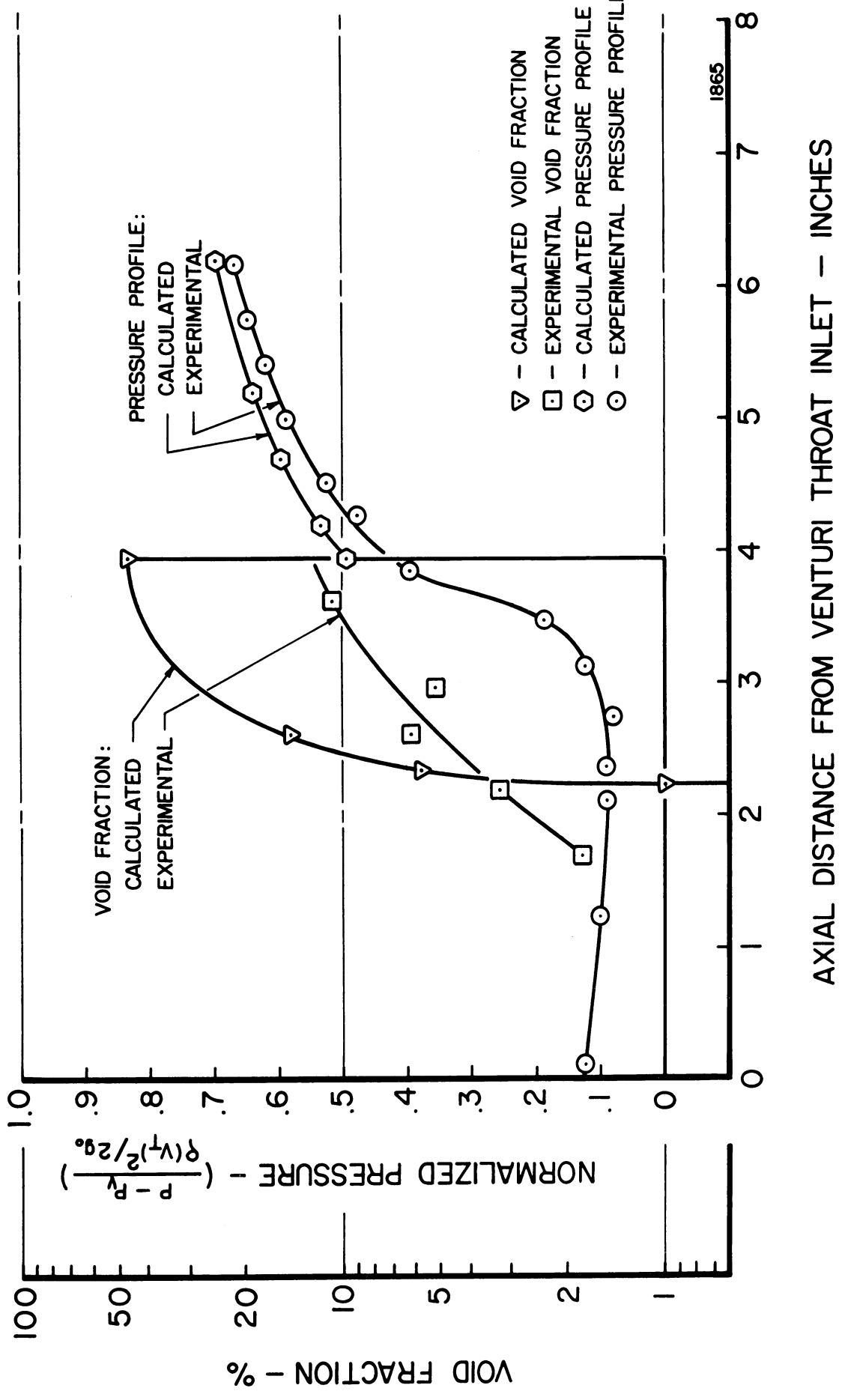

Fig. 9.--Normalized pressure and void fraction versus axial position for water, experimental versus calculated comparison for first mark cavitation.

3. Cavitation Termination to Venturi Discharge

The calculation for this region is identical to that already discussed for the shock wave model.

IV. RESULTS

A. Theoretical Models

As previously discussed, calculations have been made for the venturi shown in Fig. 1 for water at 53.5°F, 60.0°F, and 200°F. The lower temperature matches experimental water data with 64.6 ft./sec. throat velocity for void fraction and pressure profiles (15,16) taken for two different extents of the cavitating region: 0.786 inches (standard cavitation), and 1.75 inches (first mark cavitation), downstream from the throat exit.

The calculating procedures have already been described, and the equations involved are shown in the Appendix. An examination of these will show that the calculations are independent of throat velocity unless actual magnitudes of pressure rise and Mach number are required. The fluid properties, however, are required immediately, so that it is necessary to specify the fluid and its temperature. Assuming, then, that water is the fluid at the three specified temperatures and assuming various values for the ratio of cross-sectional areas between cavitation termination and throat, it is possible to compute quality, void fraction, and sonic velocity immediately upstream of the shock. For a given water temperature, there is of course a unique relation between void fraction and sonic velocity, and also void fraction and quality, and

these are shown in Figs. 3 and 4, respectively, and listed in Table I.

It is also possible, without specifying velocity, to compute the ratio of Mach numbers (M_1/M_2) across the shock and the ratio of shock pressure rise to throat kinetic pressure utilizing either of the calculational models. As noted, the Mach number ratio is very large compared to conventional compressible gas cases, increasing from the order of 10 to the order of 10^3 as the void fraction increases from the order of 10^{-4} to 10^{-1}. Even larger ratios occur as void fraction approaches unity. However, these may not be meaningful since, as previously mentioned, the assumptions made restrict the validity of the calculation to the relatively low quality range. Also both M_1/M_2 and $(p_2/p_v)/\rho V_t^2$ decrease markedly as void fraction is decreased, and become unity for zero void fraction, since a condensation shock is not possible in that case.

To obtain either actual Mach numbers or pressure rise, it is necessary to specify the actual throat velocity.

B. Comparison with Experimental Data

1. Axial Pressure Profiles

Experimental axial pressure profiles have been measured (16) for the venturi of Fig. 1 for water at 53.5°F, throat velocity of 64.6 ft./sec., and for the cavitation terminating at 0.786" and 1.75", respectively, from the throat exit. For comparison with the theoretical models, a normalized suppression pressure is formed by subtracting vapor pressure and dividing the result by the throat kinetic pressure.

According to classical conceptions of cavitation, this number should always be zero at throat discharge. The fact that it normally is not is now well recognized (21, e.g.). However, the assumptions of the theoretical models are such that the normalized suppression pressure must be zero at this point. For either theoretical model the pressure is then essentially constant to the end of the cavitation region, while in the real case it falls to a minimum downstream of the throat exit (Figs. 8 and 9).

Similar pressure profile data is available for mercury (22) at a velocity of 33.1 ft./sec. and 115°F, and for the cavitation terminating at 0.786" from the throat exit. This data was normalized as previously described. The resulting comparison to the theoretical profiles is shown in Fig. 10.

At the end of the cavitation zone the theoretical models each predict a step rise in pressure, which goes through a maximum for increasing extent of the cavitation region. It can be shown from eq. (17) of Appendix C, which applies to the hydraulic jump model, that this maximum occurs for a value of venturi radius, r, equal to $(2)^{1/2} r_t$, where r_t is the venturi throat radius. The experimental profiles do not show a step rise in pressure at the end of the cavitation region (which is marked in Figs. 8, 9, and 10 by the step rise of predicted pressure), but they do show a substantial gradient of about the correct magnitude to match the prediction from the models.

After the cavitation termination region the pressure continues to rise more gradually for both experimental and theoretical profiles as

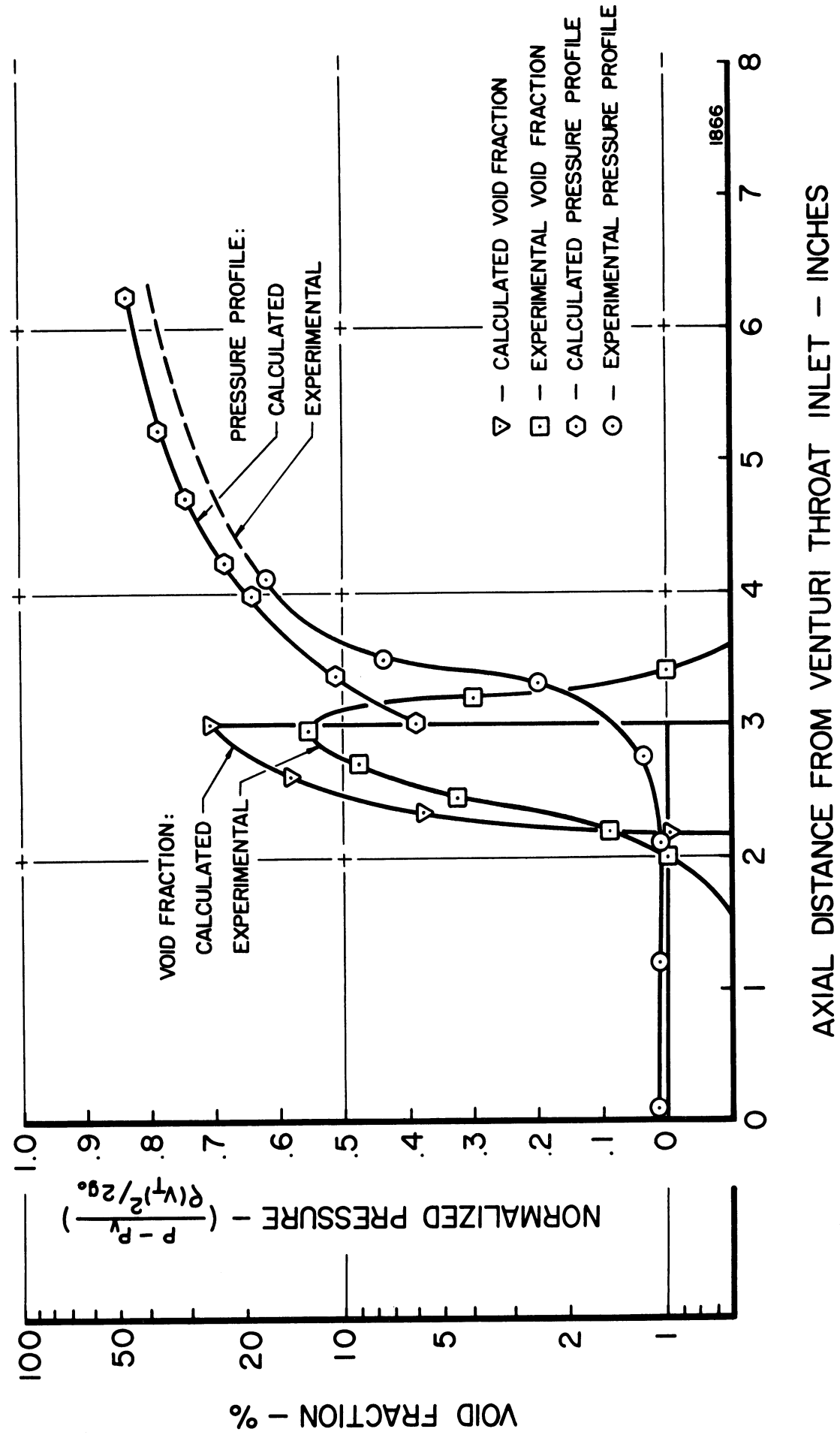

Fig. 10.--Normalized pressure and void fraction versus axial position for mercury, experimental versus calculated comparison for standard cavitation.

expected for a single phase diffuser. Thus the theoretical and experimental axial pressure profiles match reasonably well.

2. Void Fraction Profiles

Local void fractions for the flow regimes considered here was measured as a function of radius and axial position with a gamma-ray densitometer (13,15). Figs. 11 and 12 show the resulting profiles for water and Fig. 13 for mercury. For the water tests the void fraction is greatest in regions along the venturi axis, contrary to previous expectations from similar measurements and visual observations in mercury as well as earlier pitot tube measurements in water (to be discussed later). For the mercury tests it was found that the void fraction was very high along the venturi wall and small along the axis, indicating the suitability of the hydraulic jump analogy for this case.

From profiles of this type it is possible to compute average void fraction as a function of axial distance. Such profiles are shown for water and mercury for standard cavitation in Fig. 14. This, plus additional data for first mark cavitation, is replotted in Figs. 8, 9, and 10 to show the comparison with calculated values for the two flow models. While the local void fraction distributions between water and mercury differ widely, it is noted that the averaged distributions in both cases are considerably lower than the calculated models would indicate near the end of the cavitation termination region. It is noted that the void fraction distribution in mercury follows that calculated quite closely almost to the point of the jump, indicating that the hydraulic jump analogy in this case may be quite good. However, the

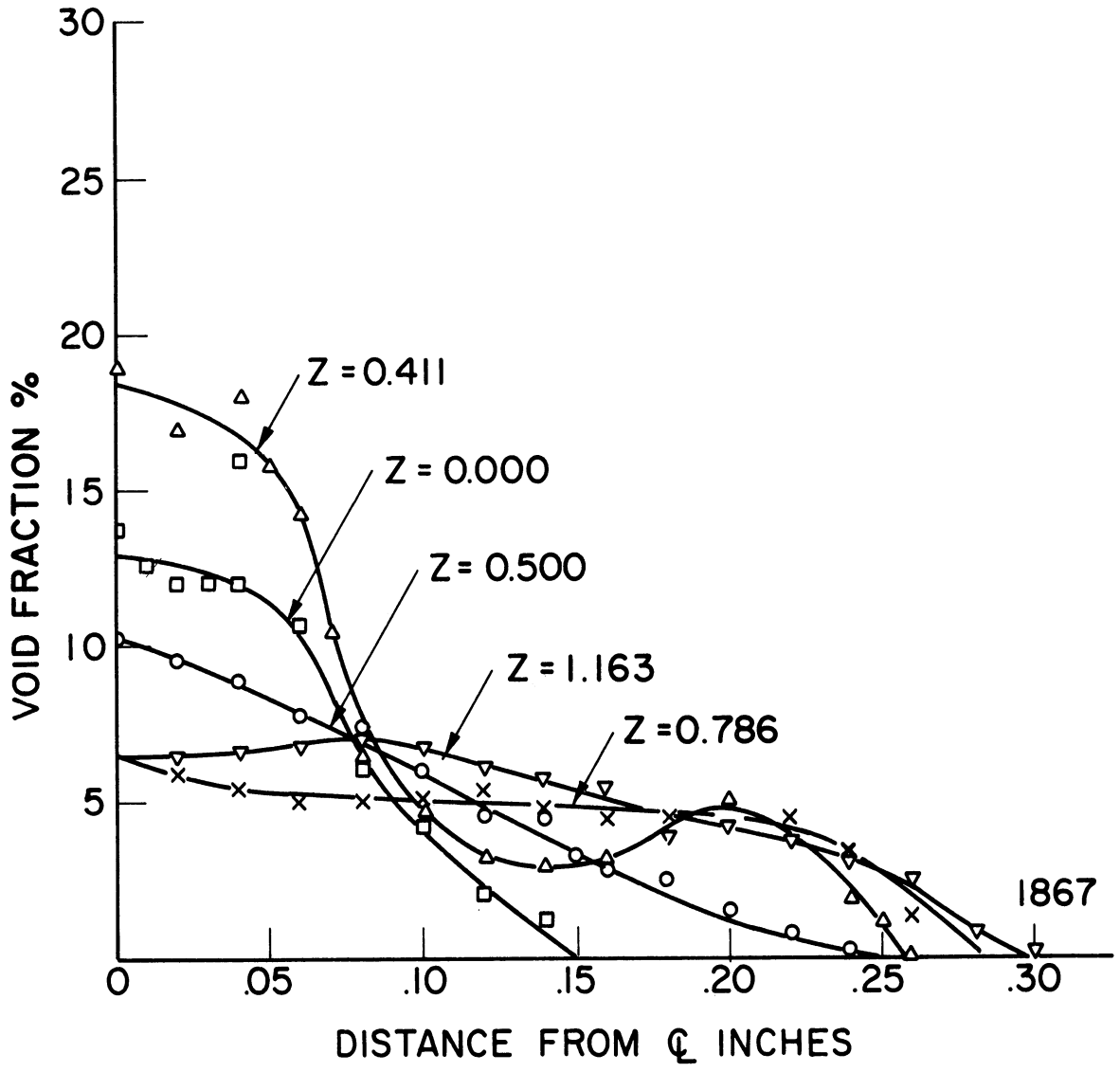

Fig. 11.--Void fraction versus radius for water at several axial locations for standard cavitation.

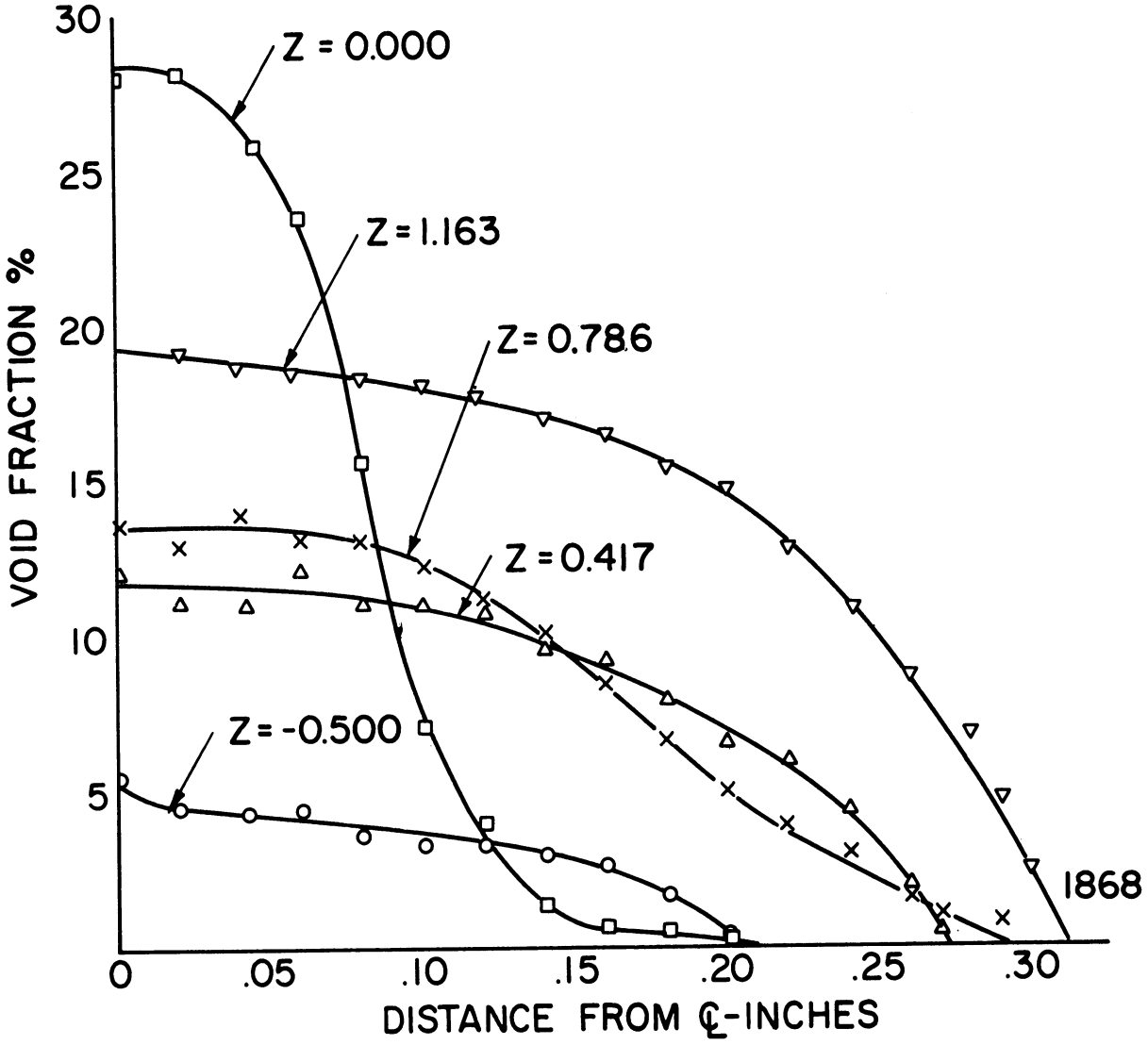

Fig. 12.--Void fraction versus radius for water at several axial locations for first mark cavitation.

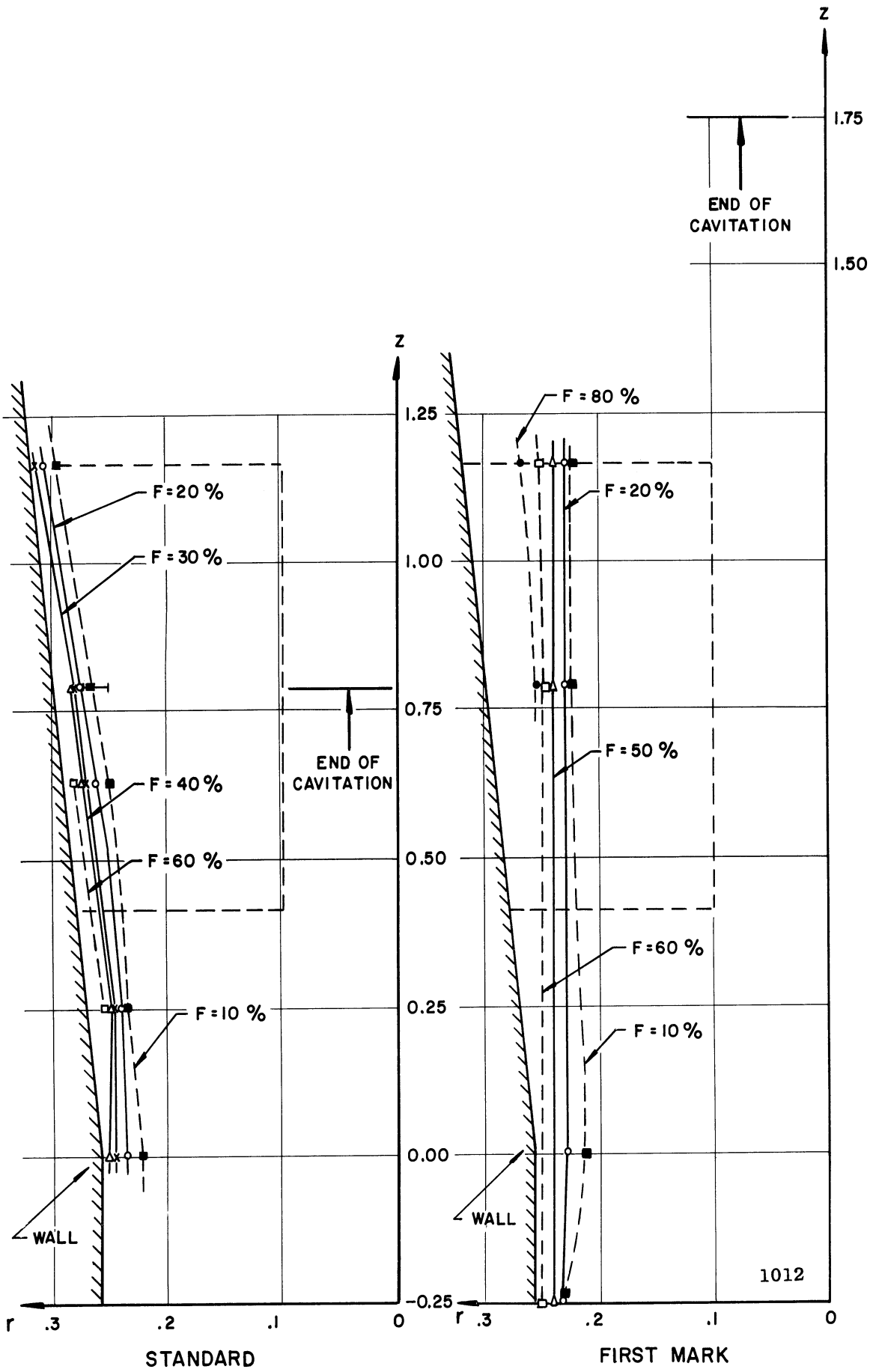

Fig. 13.--Void fraction profiles for standard and first mark cavitation conditions in mercury.

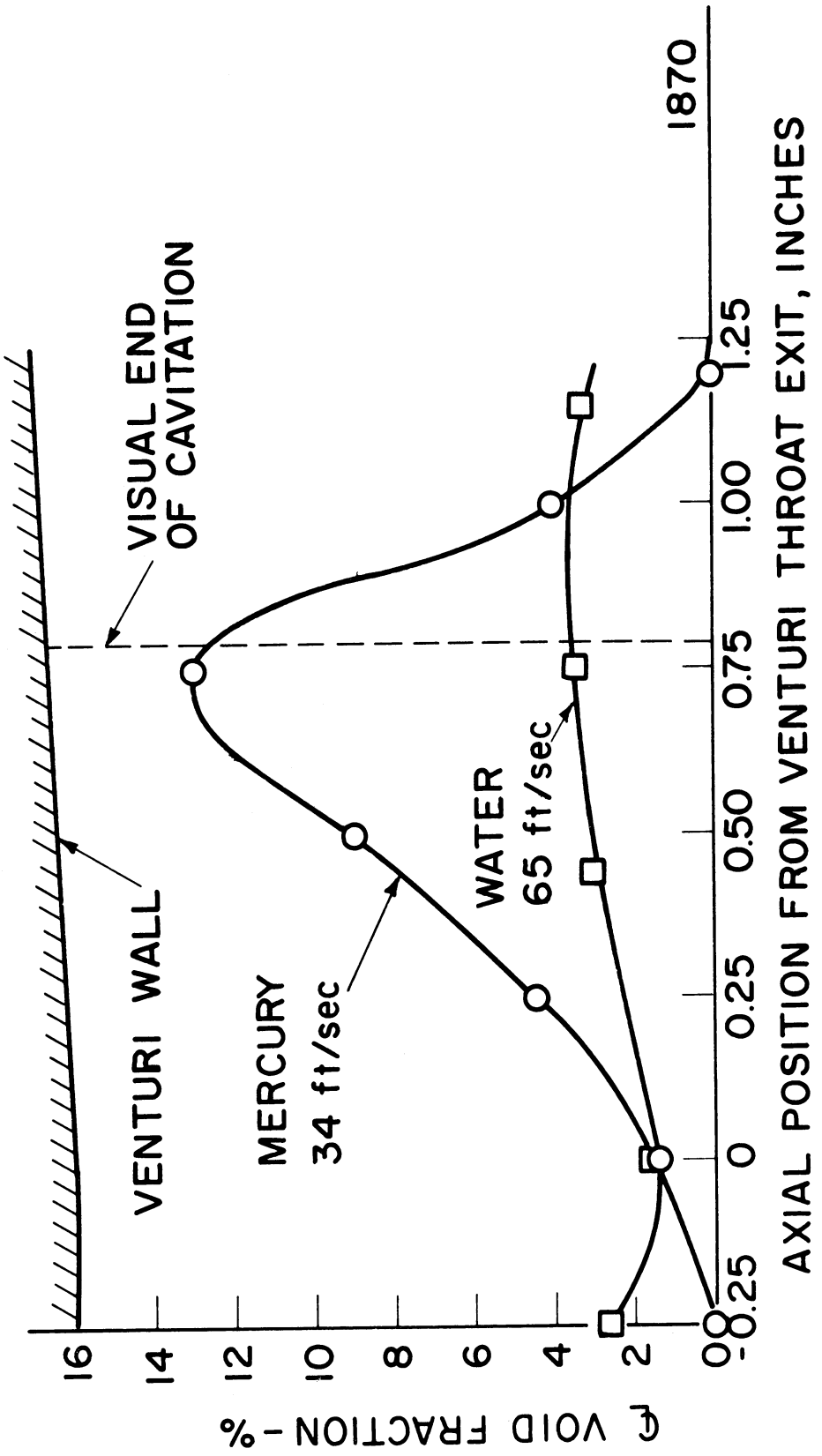

Fig. 14.--Average venturi void fraction versus axial distance for mercury.

averaged void fraction near the jump is quite a bit higher in both models than the experimental values. This is partially due to the fact that these models assume in one case that the velocity of the vapor is zero and in the other that it is equal to liquid velocity, whereas in actuality there may be significant "slip" so that the vapor velocity is considerably greater than that of the liquid. If this were the case, the void fraction for a given quality would be less, and thus somewhat nearer the experimental values.

3. Pitot Tube Measurements

Fig. 15 shows micropitot tube velocity profiles for water (21,13) across a venturi similar to that used in these tests. The pitot tube is located upstream of the cavitation termination point for two of the cavitation conditions shown (except "no cavitation" and first mark), at a point about 2 3/8" downstream from the throat exit. It is clear that in this case a well-defined central liquid jet existed with a velocity of 90 to 95% of throat velocity. That the impact pressure was the order of 90% that corresponding to throat velocity indicates that the fluid density must have been close to that of pure liquid.

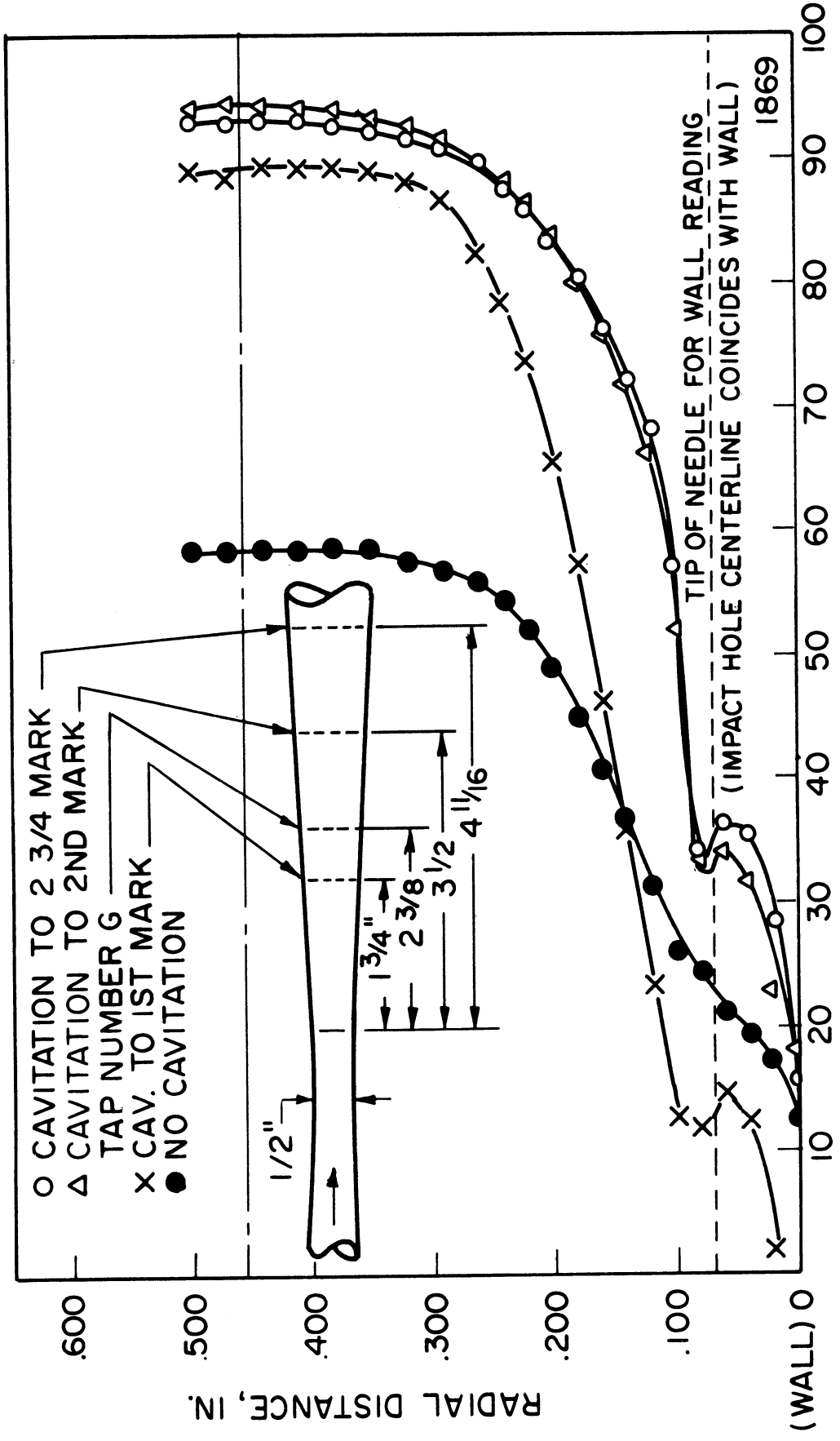

Fig. 15.--Velocity profiles as function of radial position and cavitation condition, observer at tap position G, cold water, 1/2 inch test section.

V. CONCLUSIONS

Major conclusions from this work follow:

1) Either the homogeneous flow, thermal equilibrium model or the hydraulic jump model are capable of predicting axial pressure distribution in a cavitating venturi quite closely, even including the behavior of the condensation shock marking the downstream termination of the cavitation zone. This has been verified in water and mercury.

2) Both models predict void fractions in both fluids, averaged over the cross-section at fixed axial positions, that are considerably higher than those measured by gamma-ray densitometry. This may be due to the fact that neither model allows a vapor velocity greater than the liquid velocity, whereas in actuality such a positive "slip" probably does exist.

VI. APPENDIX

A. Sonic Velocity in Low Quality Two Phase Mixtures

The sonic velocities were computed following the methods of Jakobsen (4). The operative equations are as follows:

$$a = a_l \sqrt{\frac{(1+B)^2}{(1+Bv_f/v_g)(1+B\Gamma)}} \tag{1}$$

where,

$$B = \frac{V_v}{V_L} \simeq \frac{V_v}{V_{total}} \simeq \text{Void Fraction } (= \text{V.F.}) \tag{2}$$

$$\Gamma = \frac{\rho_L a_L^2}{\rho_v a_v^2} = (v_g/v_f)(a_L/a_v)^2 \tag{3}$$

$$a_v = (g_o kRT)^{1/2} = 59.9(T)^{1/2} \text{ for water} \tag{4}$$

Equation (1) is derived in reference 4 starting with the basic relation:

$$a^2 = \left(\frac{\partial p}{\partial \rho}\right)_T \tag{5}$$

and assuming constant temperature with no evaporation or condensation during the sonic disturbance. The first assumption tends to give higher sonic velocities than the alternative assumption of thermal equilibrium,

while the second assumption tends in the opposite direction, but probably to a lesser extent.

B. Condensation Shock Wave Analysis (Assuming x = 0 after shock and $p = p_v$ before shock)

1. Basic Conservation Relations

Mass:
$$V_1 \left[v_f(1-x)+v_g x \right]^{-1} = V_2/v_f \tag{6}$$

Momentum:
$$(p_2-p_1)A = (\dot{m}/g_o)(V_1-V_2) \quad ; \quad \dot{m} = V_2 \rho_L A$$

or
$$p_2-p_1 = (\rho_L/g_o)(V_2V_1 - V_2^2) \tag{7}$$

Energy:
$$h_o = h_{l_g} x + h_{l_f}(1-x) + V_1^2/2g_oJ$$
$$= h_{2_f} + V_2^2/2g_oJ \tag{8}$$

2. Assumptions and Rearrangement to Working Form

$x = m_v/m_T = m_v/m_L$, for low quality ($x \lesssim .01$)

then,
$$x = (V_v/V_L)(\rho_v/\rho_L) = B(v_f/v_g) \tag{9}$$

For the cavitation problem, $x \ll 1$, so $1-x \simeq 1$

then (6) becomes:
$$V_1/(v_f+v_fB) = V_2/v_f = V_1/v_f(B+1)$$

or
$$V_1/V_2 = B + 1 \tag{10}$$

Introduce Mach number:

$$M_1 = V_1/a_1 \ , \ V_1 = M_1 a_1 \ , \ \text{etc.} \tag{11}$$

then (10) becomes:

$$M_1/M_2 = (a_L/a_1)(B+1)$$

Substituting for a_1 from (1):

$$M_1/M_2 = \sqrt{(1+B\Gamma)(Bv_f/v_g + 1)} \tag{12}$$

And momentum equation (7) becomes:

$$p_2-p_1 = p_2-p_v = (M_1M_2a_1a_L - M_2^2a_L^2)/g_ov_f$$

or

$$p_2 = p_v + M_2^2\left[((M_1/M_2)(a_1a_L) - a_L^2)/144g_ov_f\right] \tag{13}$$

And from (1) and (12):

$$a_1 = a_L(1+B)/\sqrt{(1+Bv_f/vg)(1+B\Gamma)} = a_L\,(1+B)/(M_1/M_2) \tag{14}$$

C. Hydraulic Jump Model (Assuming space around jet to be filled with stagnant vapor and jet static pressure = p_v)

Mass: $$V_1 \rho_L \pi r_1^2 = V_2 \rho_L \pi r_2^2$$

or

$$V_1 = V_2(r_2/r_1)^2 \tag{15}$$

Momentum:

$$F = (p_2-p_v)\pi r_2^2 = (\dot{m}/g_o)(V_1-V_2)$$
$$= (V_2 \rho_L \pi r_2^2/g_o)(V_1-V_2) \tag{16}$$

or

$$p_2-p_v = \frac{\rho_L V_2^2}{g_o}\left[\left(\frac{r_2}{r_1}\right)^2 - 1\right] \tag{17}$$

BIBLIOGRAPHY

1. Hunsaker, J. C., "Cavitation Research, A Progress Report on Work at the Massachusetts Institute of Technology," Mechanical Engineering, April, 1935, pp. 211-216.

2. Randall, L. N., "Rocket Applications of the Cavitating Venturi," ARS Journal, January-February, 1952, pp. 28-31.

3. Nowotny, H., "Destruction of Materials by Cavitation," VDI-Verlag, Berlin, Germany, 84, 1942. Reprinted by Edwards Brothers, Inc., Ann Arbor, Michigan, 1946. English language translation as ORA Internal Report No. 03424-15-I, Department of Nuclear Engineering, The University of Michigan, 1962.

4. Jakobsen, J. K., "On the Mechanism of Head Breakdown in Cavitating Inducers," Trans. ASME, J. Basic Eng., June 1964, pp. 291-305.

5. Spraker, W. A., "Two-Phase Compressibility Effects on Pump Cavitation," Cavitation in Fluid Machinery, ASME, 1965, pp. 162-171.

6. Muir, J. F., and Eichorn, R., "Compressible Flow of an Air-Water Mixture Through a Vertical Two-Dimensional Converging-Diverging Nozzle," Proc. 1963 Heat Transfer and Fluid Mechanics Institute, pp. 183-204.

7. Starkman, E. S., Schrock, V. E., Neusen, K. F., Maneely, D. J., "Expansion of a Very Low-Quality Two-Phase Fluid Through a Convergent-Divergent Nozzle," J. Basic Eng., Trans. ASME, June, 1964, pp. 247-264.

8. Eddington, R. B., "Investigations of Shock Phenomena in a Supersonic Two-Phase Tunnel," AIAA Paper No. 66-87, 3rd Aerospace Sciences Meeting, New York, January, 1966.

9. Levy, S., "Prediction of Two-Phase Critical Flow Rate," ASME Paper 64-HT-8, J. Heat Transfer, Trans. ASME, May, 1960, p. 113.

10. Moody, F. J., "Maximum Flow Rate of a Single Component, Two-Phase Mixture," ASME Paper 64-HT-35, ASME Trans., J. Heat Transfer.

11. Min, T. C., Fauske, H. K., Petrick, M., "Effect of Flow Passages on Two-Phase Critical Flow," I&EC Fundamentals, Vol. 5, No. 1, February, 1966, pp. 50-55.

12. Deich, M. E., Stepanchuk, V. F., Saltanov, G. A., "Calculating Compression Shocks in the Wet Steam Region," Teploenergetika, 1965, 12 (4), pp. 81-84.

13. Smith, W., Atkinson, G. L., Hammitt, F. G., "Void Fraction Measurements in a Cavitating Venturi," Trans. ASME, J. Basic Eng., June, 1964, pp. 265-274.

14. Hammitt, F. G., Smith, W., Lauchlan, I., Ivany, R., and Robinson, M. J., "Void Fraction Measurements in Cavitating Mercury," ANS Trans., Vol. 7, No. 1, pp. 189-190; also Nuclear Applications, February, 1965, pp. 62-68.

15. Lauchlan, I. E. B., "Void Fraction Measurements in Water," Term Paper, NE-690, Nuclear Engineering Department, The University of Michigan, Ann Arbor, Michigan, August, 1963.

16. Ericson, D. M., Jr., Capt. USAF, unpublished data, Thesis underway, Nuclear Engineering Department, The University of Michigan, 1964.

17. Hammitt, F. G., "Cavitation Damage and Performance Research Facilities," Symposium on Cavitation Research Facilities and Techniques, pp. 175-184, ASME Fluids Engineering Division, May, 1964.

18. Hammitt, F. G., Wakamo, C. L., Chu, P. T., Cramer, V. L., "Fluid-Dynamic Performance of a Cavitating Venturi," ORA Technical Report No. 03424-2-T, Nuclear Engineering Department, The University of Michigan, October, 1960.

19. Keenan, J. H., Keyes, F. G., Thermodynamic Properties of Steam, John Wiley & Sons, Inc., New York, New York, Thirtieth Printing, April, 1957.

20. Streeter, V. L., Fluid Mechanics, McGraw-Hill, 1958.

21. Hammitt, F. G., "Observation of Cavitation Scale and Thermodynamic Effects in Stationary and Rotating Components," J. Basic Eng., Trans. ASME, p. 1, 1963.

22. Robinson, M. J., "On the Detailed Flow Structure and the Corresponding Damage to Test Specimens in a Cavitating Venturi," Ph.D. Thesis, Nuclear Engineering Department, The University of Michigan, August, 1965.